



HAL
open science

Properties of pendular liquid bridges determined on Delaunay's roulettes

Boleslaw Mielniczuk, Olivier Millet, Gérard Gagneux, Moulay Said El
Youssoufi

► **To cite this version:**

Boleslaw Mielniczuk, Olivier Millet, Gérard Gagneux, Moulay Said El Youssoufi. Properties of pendular liquid bridges determined on Delaunay's roulettes. *Powders & Grains 2017*, Jul 2017, Montpellier, France. 10.1051/epjconf/201714009042 . hal-01667641

HAL Id: hal-01667641

<https://hal.umontpellier.fr/hal-01667641v1>

Submitted on 19 Dec 2017

HAL is a multi-disciplinary open access archive for the deposit and dissemination of scientific research documents, whether they are published or not. The documents may come from teaching and research institutions in France or abroad, or from public or private research centers.

L'archive ouverte pluridisciplinaire **HAL**, est destinée au dépôt et à la diffusion de documents scientifiques de niveau recherche, publiés ou non, émanant des établissements d'enseignement et de recherche français ou étrangers, des laboratoires publics ou privés.

Properties of pendular liquid bridges determined on Delaunay's roulettes

Boleslaw Mielniczuk^{1,2,*}, Olivier Millet¹, Gérard Gagneux¹, and Moulay Said El Youssoufi^{2,3}

¹LaSIE, UMR-CNRS 7356, University of La Rochelle, 17042 La Rochelle Cedex 1, France.

²LMGC UMR CNRS 5508, University of Montpellier, 34095 Montpellier Cedex 5, France.

³Laboratory MIST, IRSN-CNRS-University of Montpellier, France.

Abstract. This work addresses the study of capillary bridge properties between two grains, with use of recent analytical model, based on solutions of Young-Laplace equation from an inverse problem. A simple explicit criterion allows to classify the profile of capillary bridge as a surface of revolution with constant mean curvature (Delaunay roulette) using its measured geometrical parameters (gorge radius, contact angle, half-filling angle). Necessary data are obtained from experimental tests, realized on liquid bridges between two equal spherical grains. Sequences of images are recorded at several (fixed) volumes of liquid and different separations distances between the spheres (from contact to rupture), in laboratory and in micro-gravity conditions. For each configuration, an exact parametric representation of the meridian is revealed. Mean bridge curvature, internal pressure and intergranular capillary force are also determined.

1 Introduction

Capillary bridge is a liquid link between solid particles (grains). It gives origin of several phenomena observed in unsaturated granular materials, in particular of interparticle capillary force. This force contributes to the formation, deformation and flow of granular materials (soils, powders, photonic crystal production, etc.), with significant influence on mechanical and physical properties of such materials. It imparts an apparent macroscopic strength (sand castle effect) to moist granular materials, even in the absence of intrinsic cohesion or confining stress (see e.g. [1, 2]). The knowledge on the behaviour of intergranular liquid at a local scale, in different conditions, seems to be indispensable in complete description of phenomena observed in humid granular materials and in modelling of such materials.

The most elementary capillary bridge is a pendular bridge: liquid bridge between two solid grains. Shape and evolution of pendular capillary bridges have been analysed for over hundred years from theoretical and experimental point of view (see e.g. [3-7]). However, the results of numerical modelling and physical experiments are not always in good accordance, because of several simplifications and approximations introduced often into the mathematical models.

This work addresses the experimental study of capillary bridge properties with use of the recent analytical calculation of bridge profile, based on solution of

Young-Laplace equation [8]. In this method, the parameters of pendular bridge and the shape of its meridian may be estimated using appropriate theoretical solutions, based on an inverse problem, as the internal capillary pressure is unknown [8]. However, this pressure may be recovered with experimental measurements of geometrical parameters of liquid bridge: gorge radius y^* , contact angle θ , half-filling angle δ (see Fig. 1).

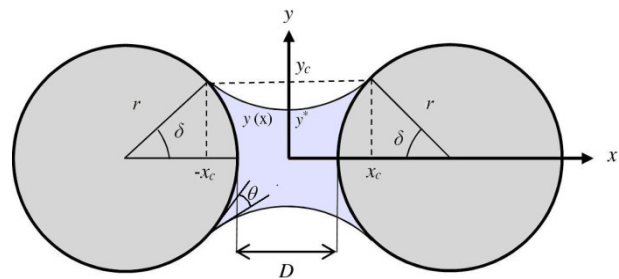


Fig. 1. Schema of capillary bridge and its main geometrical parameters.

2 Experimental setup

Experimental setup consists of photo camera, system of support which allows positioning of both grains, and background light (see Fig. 2). It is similar to configuration described in [9-11]. To examine capillary bridges in zero-gravity conditions, it is put into the rack, adapted for parabolic flight.

* Corresponding author: boleslaw.mielniczuk@umontpellier.fr

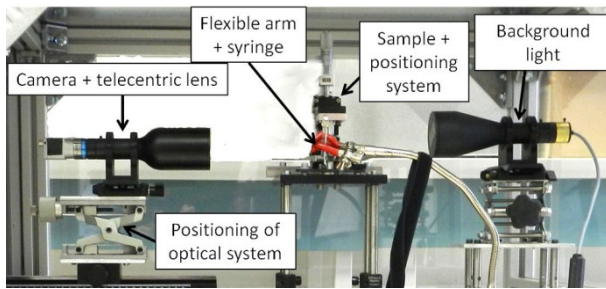


Fig. 2. Global view of experimental apparatus.

Capillary bridges between two borosilicate-glass spheres with diameter of 8 mm or 10 mm and with a fixed volume of water (from 1 to 10 μl) are examined. Initially, bridge is created for a separation distance between spheres D close to zero. Then, D is steeply increased up to the rupture of the bridge (step of 0.1 mm). For each D the photo of the capillary bridge is recorded and the geometric parameters (gorge radius y^* , half-filling angle δ , contact angle θ) are measured by image processing. Then the shape of the capillary bridge, and its exact analytical parameterization, are deduced, according to the criterion given in [8].

3 Results of laboratory tests

Experimental data are analysed for each examined configuration (D , V). Measured geometrical parameters are used to determine the type of curve, to reconstruct and trace the bridge profile and to calculate bridge characteristics. Bridge profiles are approximated as surfaces of revolution with constant mean curvature (Delaunay roulettes). Evolution of their main geometrical parameters is briefly presented below.

Gorge radius y^* decreases almost linearly with increasing separation distance D for all examined volumes, with similar evolution for both sphere diameters. For higher bridge volumes V , higher final separation distance D_r (distance at rupture) is observed, from about $D_r=1.2$ mm for $V=1$ μl , to $D_r=2.2$ mm for $V=10$ μl .

Angle δ decreases from the beginning to about 50% of final separation D_r , then it remains constant up to the rupture. The value of contact angle θ initially decreases with increasing D , but it becomes constant very soon, while half-filling angle δ is still decreasing: pinning of contact line is observed (see details in i.e. [10]).

Evolution of mean curvature of the profile H is presented in Fig. 3. It depends on volume of water V and on separation distance D and it has slightly higher values for 10mm spheres diameter. In general, H is initially positive and it decreases almost linearly with increase of separation distance. At about 70-90% of the critical separation D_r , H passes through zero, becomes negative and stays negative up to the rupture (Fig. 3).

The sign of H determines also the sign of internal pressure $\Delta p = p_i - p_g$ (Laplace pressure, difference of pressure between the interior and the exterior of the capillary bridge) and the type of Delaunay's roulette used to approximate the bridge profile (see [8, 11]).

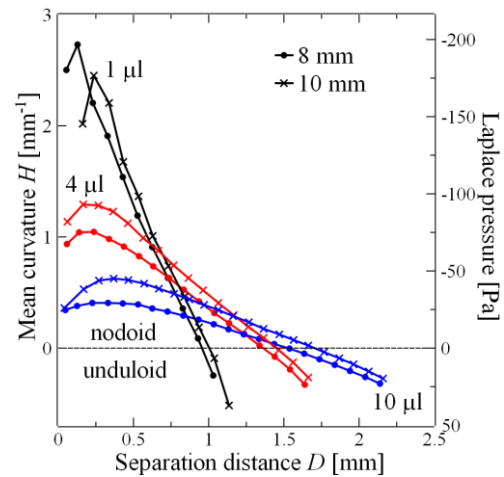
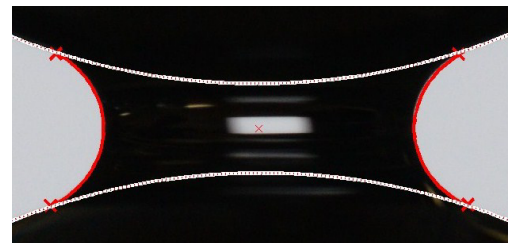
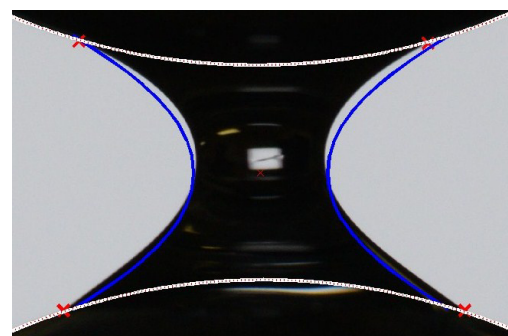


Fig. 3. Mean curvature H and internal pressure Δp of capillary bridge between spheres with diameter of 8 mm and 10 mm, as a function of separation distance D . $H > 0$ corresponds to the nodoid case and $H < 0$ to the unduloid one.

Two types of convex curves were observed in our experiments: a portion of nodoid (Delaunay hyperbolic roulette, from the creation of the capillary bridge to some distance D , $H > 0$ and $\Delta p < 0$) and a portion of unduloid (Delaunay elliptic roulette, before rupture, $H < 0$, $\Delta p > 0$).



$D = 0.66$ mm, $y^* = 1.16$ mm, $\delta = 17.85^\circ$, $\theta = 10.5^\circ$, nodoid



$D = 1.66$ mm, $y^* = 0.52$ mm, $\delta = 16.9^\circ$, $\theta = 14.8^\circ$, unduloid

Fig. 4. Resulting bridge profiles superposed on the original images for glass spheres of 10mm. The data are for fixed volume $V = 4$ μl and various distances D between grains (red: nodoid shape, blue: unduloid shape, calculated from theory).

Calculated bridge profiles are then superposed on the original photos to validate the approach, used in theoretical model. Example of sequence, obtained for capillary bridge between 10 mm spheres diameter, with $V = 4$ μl and different D are presented in Fig. 4. Calculated contact points and reconstructed bridge meridians are traced on recorded images.

Intergranular capillary force can be evaluated as $F_{cap} = F_{\Delta p} + F_{ST}$, including two contributing forces: pressure resulting force $F_{\Delta p} = \pi \gamma H y^*{}^2$ and surface tension resulting force $F_{ST} = 2\pi \gamma y^*$, where surface tension coefficient of water $\gamma = 0.072$ N/m. In general, the decrease of capillary force F_{cap} is observed with increasing D (Fig. 5). Only for 10mm spheres at $V=10 \mu\text{l}$, initial increase of F_{cap} is observed. At the moment of rupture, capillary force is higher for larger volumes of water (see Fig. 5).

For all realized tests, initially negative Δp becomes positive (with repulsive $F_{\Delta p}$) with increasing separation D . However, capillary force F_{cap} remains always attractive, because of dominating influence of attractive surface tension resulting force F_{ST} (see also [10]).

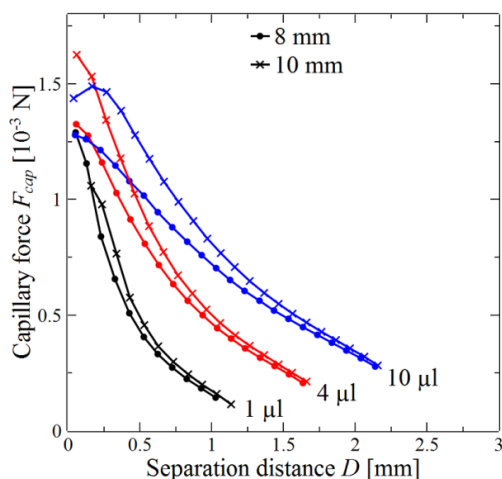


Fig. 5. Calculated capillary force F_{cap} as a function of interparticle distance D for capillary bridge between 8 and 10mm spheres diameter.

In Fig. 6, calculated F_{cap} is compared with capillary force measured in earlier experiments on extended capillary bridges, with use of laboratory balance [9, 10].

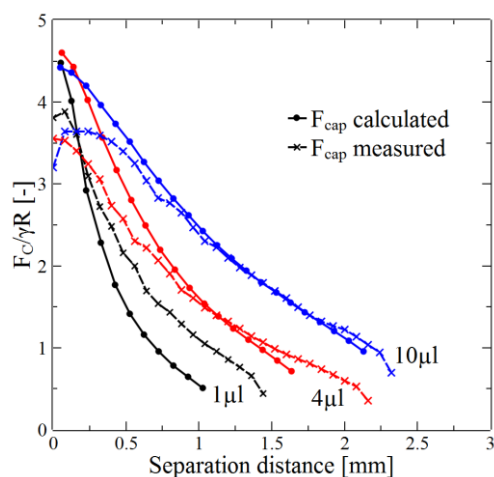


Fig. 6. Calculated and measured capillary forces F_{cap} in function of interparticle distance D for the spheres of 8 mm.

The liquids with different surface tension coefficients were used; both results are thus normalized with respect to γ , to make possible the direct comparison of measured and calculated values. The results are generally in good

accordance. Although, it is seen that for small D , calculated force is higher than measured one. With increasing D , this difference becomes smaller, while close to the rupture, the measured force becomes slightly higher than the calculated one, especially for small V . Differences in both types of results may origin from different types of tests (continuous extension or quasi-static capillary bridges) and different surface tension coefficient of used liquids.

4 Micro-gravity tests

For larger liquid volumes and/or relatively high separation distance D , water is driven towards the lower part of the bridge due to the effects of gravity and capillary bridge loses its symmetry. The importance of the influence of the gravity on the bridge shape may be estimated with use of the Bond number $Bo = \Delta \rho g r^2 / \gamma$, where $\Delta \rho$ is the difference in densities between water and air, and g is the acceleration of gravity.

The influence of gravity is negligible if $Bo / |2\xi r| \ll 1$ (where ξ is the bridge curvature) [12].

This is the case for capillary bridges containing low water volume and at low separation distance. One can see, than for such bridges, calculated profiles fits well with the ones recorded with use of photo camera.

When V becomes higher, the influence of gravity can no longer be neglected: geometry of the bridge is distorted and calculated variables are no more correct.

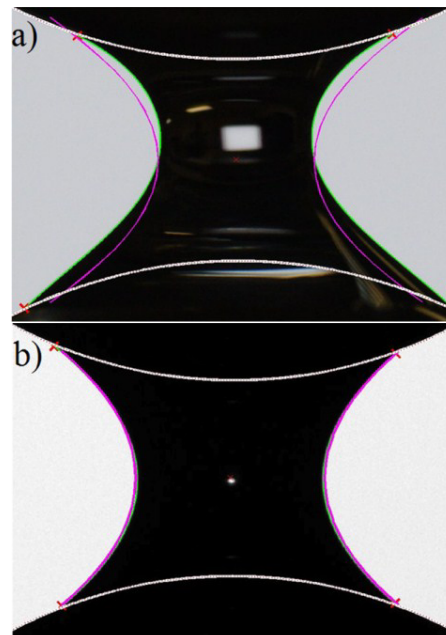


Fig. 7. Resulting bridge profiles (magenta: bridge shape, calculated from theory) superposed on the original images for capillary bridge between glass spheres of 10mm, with liquid volume $V = 10 \mu\text{l}$ and separation distance $D = 2.06$ mm, recorded in laboratory (a) and during parabolic flight (b).

An example showing the influence of gravity on a capillary bridge profile is shown in Fig. 7a). In this example, Bond number is close to 0.3 and theoretical profile is quite far from the recorded profile of the capillary bridge.

For now, taking into account the gravity in the general theoretical modelling do not allow to obtain simple analytical solution. It is therefore necessary to get rid of the effects of gravity in order to validate the modelling, carried out on a wide range of parameters (volume of the liquid bridge, grain size, separation distance, ...).

To minimize the influence of gravity, experimental tests were realized also in micro-gravity conditions, during parabolic flight (joint project between LMGC, LaSIE and CNES), with use of the same experimental protocol. Example of results obtained in micro-gravity conditions is presented in Fig. 7. Distortion of the bridge is observed in Fig. 7a) (laboratory test), while identical bridge examined during parabolic flight is not affected by the gravity (Fig. 7b).

Comparison of calculated mean curvature H and capillary force F_{cap} for capillary bridges between 8 mm spheres tested in laboratory and during parabolic flight is presented in Fig. 8.

It is seen, that calculated parameters are different for both tests, especially for higher separations D . Calculated F_{cap} (and also Δp) close to the rupture are larger for bridges tested in microgravity conditions. In addition, stability of capillary bridges is increased in such conditions and rupture of the bridge occurs at larger separations D . However, the passage by $H=0$, between two types of Delaunay's roulettes, occurs at the same separation distance for both experimental conditions.

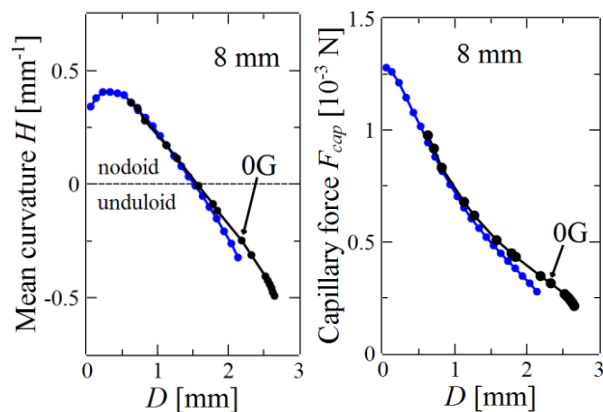


Fig. 8. Comparison of calculated mean curvature H (a) and capillary force F_{cap} (b) as a function of interparticle distance D for capillary bridges between 8mm spheres and $V=10\mu\text{l}$, in laboratory and micro-gravity tests.

5 Conclusions

In this paper we present some results of studies on capillary bridges between two equal spherical grains. Recent analytical model was used to determine variables and parameters associated with these capillary bridges. The accuracy and validity of the model was demonstrated by comparison with the experimental results. The results from theoretical modeling match very accurately experimental results for small liquid volumes and small separations between particles. For larger ones,

the capillary bridge loses its symmetry due the effects of gravity.

In order to remove the distortion effect due to gravity, experiments in micro-gravity conditions, during a parabolic flight have been performed. For these tests, theoretical results are in good agreement with experimental ones, independently of liquid volumes and/or separations distances between grains.

We found that with increasing separation distance between grains the profile of capillary bridge profile evolves from nodoid to unduloid. This passage is accompanied by the increase of internal pressure, from initially negative values to positive pressure before the rupture, while capillary force continuously decreases. Experimental validation of proposed model justifies its further development, its adaptation to other configurations of capillary bridges, including dynamic processes and analysis of stability/rupture of liquid bridges, envisaged in the nearest future.

The part of the work concerning the experiments in micro-gravity was supported by the CNES (joint project PARABOLE 2015, VP118, between LaSIE-LMGC-CNES).

References

- [1] H. Peron, J. Y. Delenne, L. Laloui, M. S. El Youssoufi, *Comput. Geotech.* **36**, 61 (2009)
- [2] H. Rahardjo, D. G. Fredlund, *Can. Geotech. J.* **32**, 749 (1995)
- [3] T. Young, *Phil. Trans.* **95**, 64 (1850)
- [4] G. Mason, W. C. Clark, *Chem. Eng. Sci.* **20**, 859 (1965)
- [5] G. Lian, C. Thornton, M. J. Adams, *J. Colloid Interf. Sci.* **161**, 138 (1993)
- [6] Ch. D. Willett, M. J. Adams, S. A. Johnson, J. P. K. Seville, *Langmuir* **16**, 9396 (2000)
- [7] F. Soulié, F. Cherblanc, M. S. El Youssoufi, C. Saix, *Int. J. Numer. Anal. Meth. Geomech.* **30**, 213 (2006)
- [8] G. Gagneux, O. Millet, *Transport Porous Med.* **105**, 117 (2014)
- [9] B. Mielniczuk, T. Hueckel, M. S. El Youssoufi, *Gran. Matt.* **16**, 815 (2014)
- [10] B. Mielniczuk, T. Hueckel, M. S. El Youssoufi, *Powder Technol.* **283**, 131 (2015)
- [11] G. Gagneux, O. Millet, B. Mielniczuk, M. S. El Youssoufi, *Eur J Environ Civ En.*, 10.1080/19648189.2016.1167782 (2016)
- [12] M. J. Adams, S. A. Johnson, J. P. K. Seville, and C. Willett, *Langmuir* **18**, 6180 (2002)